

# Bayesian assessment of chlorofluorocarbon (CFC), hydrochlorofluorocarbon (HCFC) and halon banks suggest large reservoirs still present in old equipment

Megan Lickley<sup>1</sup>, John Daniel<sup>2</sup>, Eric Fleming<sup>3,4</sup>, Stefan Reimann<sup>5</sup>, Susan Solomon<sup>1</sup>

1. Department of Earth, Atmospheric and Planetary Sciences, Massachusetts Institute of Technology, Cambridge, MA 02139, USA
2. NOAA Chemical Sciences Laboratory (CSL), Boulder, CO 80305-3328, USA
3. NASA Goddard Space Flight Center, Greenbelt, MD, USA
4. Science Systems and Applications, Inc., Lanham, MD, USA
5. Laboratory for Air Pollution/Environmental Technology, Empa, Swiss Federal Laboratories for Materials Science and Technologies, Dübendorf, Switzerland

*Correspondence to:* Megan Lickley ([mlickley@mit.edu](mailto:mlickley@mit.edu))

## Abstract

Halocarbons contained in equipment such as air conditioners, fire extinguishers, and foams continue to be emitted after production has ceased. These ‘banks’ within equipment and applications are thus potential sources of future emissions, and must be carefully accounted for in order to evaluate nascent production versus banked emissions. Here, we build on a probabilistic Bayesian model, previously developed to quantify CFC-11, 12 and 113 banks and their emissions. We extend this model to a suite of the major banked chemicals regulated under the Montreal Protocol (HCFC-22, HCFC-141b, and HCFC-142b, halon-1211, and halon-1301, and CFC-114 and CFC-115) along with CFC-11, 12 and 113 in order to quantify a fuller range of ozone-depleting substance banks by chemical and equipment type. We show that if atmospheric lifetime and prior assumptions are accurate, banks are very likely larger than previous international assessments suggest, and that total production has been very likely higher than reported. We identify that banks of greatest climate-relevance, as determined by global warming potential weighting, are largely concentrated in CFC-11 foams and CFC-12 and HCFC-22 non-hermetic refrigeration. Halons, CFC-11, and 12 banks dominate the banks weighted by ozone depletion potential. Thus, we identify and quantify the uncertainties in substantial banks whose future emissions will contribute to future global warming and delay ozone hole recovery if left unrecovered.

## 1. Introduction

The Montreal Protocol regulates the production of ozone-depleting substances (ODPs), and its implementation has avoided a world with catastrophic stratospheric ozone depletion (Newman et al., 2009). Globally, there has been a near-cessation of chlorofluorocarbon (CFC) and halon production since 2010, and global production of the replacement hydrochlorofluorocarbons (HCFCs), are scheduled to be phased-out by 2030. Despite production phase-out, these chemicals persist in old equipment produced prior to phase-out, such as refrigeration, air conditioners, foams, and fire extinguishers. These reservoirs of materials (termed ‘banks’) continue to be sources of emissions (e.g., WMO, 2018). Previously published estimates of bank sizes and bank emissions vary widely due to different estimation techniques that incorporate incomplete or imprecise information (TEAP, 2009; WMO, 2003). This uncertainty obscures

47 ongoing emissions attribution and undermines international efforts to evaluate global compliance  
48 with the Montreal Protocol. In earlier work, Lickley et al. (2020, 2021) developed a Bayesian  
49 probabilistic banks model for CFCs that incorporates the widest range of constraints to date  
50 (Lickley et al., 2020, 2021). Here, we extend this model to the suite of major chemicals  
51 regulated by the Protocol that are subject to banking.

52 Previously published assessments typically rely on one of three modeling approaches to  
53 estimate bank sizes and to then estimate emissions associated with these banks. In the “top-  
54 down” approach (e.g. WMO, 2003), banks are estimated as the cumulative difference between  
55 reported production and observationally-derived emissions. However, by taking the cumulative  
56 sum of a small difference between two large values, small biases in emissions or reported  
57 production estimates can propagate into large biases in bank estimates (Velders & Daniel, 2014).  
58 Some type of bias is thus expected since total production has very likely been less than reported  
59 production both due to under-reporting of production (e.g. Gamlen et al., 1986; Montzka et al.,  
60 2018) and due to the exclusion of point of production losses in reported production values.  
61 Further, emissions estimates rely on observed concentrations along with global lifetime  
62 estimates, which have large uncertainties associated with them (SPARC, 2013).

63 The second approach relies on a “bottom-up” accounting method (Ashford et al., 2004;  
64 IPCC/TEAP, 2006), where the inventory of sales by equipment type are carefully tallied along  
65 with estimated release rates by application use. The bottom-up approach also relies on sales data  
66 from surveys of various equipment types and products as well as estimates of their respective  
67 leakage rates (SROC, 2005). These are all subject to uncertainties, which contributes to  
68 uncertainties in bottom-up bank estimates as well. A limitation of the bottom-up method is that  
69 observed atmospheric concentrations are used only as a qualitative check and are not explicitly  
70 accounted for in the analysis. Another important limitation is that data used in the bottom-up  
71 accounting method are unobserved but rather rely on estimated processes along with reported  
72 data, such as production or sales of equipment, thus bias in reporting could propagate into large  
73 biases in bank estimates.

74 The third approach, and the one used in more recent ozone assessments (WMO, 2011, 2014,  
75 2018) uses a hybrid approach to calculate banks. Bottom-up banks estimated for 2008 are used  
76 as the starting point of the calculations. These banks are taken from SROC (2006) and represent  
77 interpolated values from the 2002 and 2015 estimates. The banks are then brought forward to the  
78 present time by adding the cumulate reported production and subtracting the cumulative  
79 observationally-derived emission from 2008 through the present. This approach is consistent  
80 with 2008 bottom-up bank estimates by design, however, as time between 2008 and the present  
81 has grown, the cumulative errors associated with the top-down approach have become larger.

82 The modeling approach applied in the present study relies on Bayesian inference of  
83 banks (Lickley et al., 2020, 2021) where banks are estimated using an approach called Bayesian  
84 parameter estimation. In this approach a simulation model of the bottom-up method is  
85 developed, where prior distributions of input parameters are constructed from previously  
86 published values, accounting for large uncertainties in production and bank release rates. The  
87 simulation model simultaneously models banks, emissions, and atmospheric concentrations.  
88 Parameters in the simulation model are then conditioned (or updated) on observed concentrations  
89 by applying Bayes’ theorem. The final result is a posterior distribution of banks by chemical and  
90 equipment type, along with an updated estimate of production and release rates for each  
91 equipment type. This approach incorporates data and assumptions from both the bottom-up and

92 top-down approaches, providing a simulation model consistent with the bottom-up accounting  
93 approach while also being consistent with observed concentrations within their uncertainties.

94 The remainder of the paper includes the following: Section 2 presents the Bayesian modeling  
95 approach along with data used in the analysis. Section 3 provides a summary of the results of  
96 our analysis for each of the chemicals considered here. Finally, Section 4 provides a discussion  
97 of our primary findings and limitations of the analysis.

## 98 99 **2. Methods**

100  
101 The Bayesian modeling approach from Lickley et al. (2020, 2021) draws on a Bayesian analysis  
102 approach called Bayesian melding, designed by Poole & Raftery (2000), that allows us to apply  
103 inference to a deterministic simulation model. We employ a version of this method that we  
104 henceforth refer to as Bayesian Parameter Estimation (BPE), which allows for input parameter  
105 uncertainty (Bates et al., 2003; Hong et al., 2005). The model flow is implemented as follows;  
106 first we develop a deterministic simulation model, representing the “bottom-up” accounting  
107 method that simultaneously simulates banks, emissions, and mole fractions for each chemical  
108 and equipment type. In this analysis, the chemicals considered include CFC-11, 12, 113, 114,  
109 and 115, HCFC-22, 141b, and 142b, and halon-1201, and 1311. Prior distributions for each of  
110 the input parameters are based on previously published estimates. We then specify the  
111 likelihood function as a function of the difference between observed and simulated mole  
112 fractions. Finally, we estimate posterior distributions of both the input and output parameters by  
113 implementing Bayes’ Rule using a sampling procedure. Each of the steps of the BPE are  
114 described in more detail below.

### 115 116 **2.1 Simulation Model**

117 The simulation model is comprised of equations (1) – (5) which simultaneously models banks,  
118 emissions, and mole fractions for each chemical by equipment type for all years with available  
119 data up until 2019. Starting dates differ by chemical, see the Supplement for details. The  
120 simulation model is specified as follows;

$$121  
122 B_{j,t+1} = (1 - RF_{j,t}) \times B_{j,t} + (1 - DE_{j,t}) \times P_{j,t} \quad (1)$$

123  
124 where  $B_{j,t}$ , is banks and  $P_{j,t}$  is production of equipment category,  $j$ , in year,  $t$ .  $RF_{j,t}$  reflects the  
125 fraction of the bank released and  $DE_{j,t}$  reflects the fraction of production that is directly emitted  
126 in equipment category,  $j$ , year,  $t$ . These same parameters are used to simulate emissions,  $E_{j,t}$ :

$$127  
128 E_{j,t+1} = RF_{j,t} \times B_{j,t} + DE_{j,t} \times P_{j,t} \quad (2)$$

129  
130 Total banks,  $B_{\text{Total},t}$ , and total emissions,  $E_{\text{Total},t}$ , are then estimated as the sum across all  $N$   
131 equipment categories;

$$132  
133 B_{\text{Total},t} = \sum_{j=1}^N B_{j,t} \quad (3)$$

$$134  
135 E_{\text{Total},t} = \sum_{j=1}^N E_{j,t} \quad (4)$$

136

137 For chemicals where feedstock usage is reported, an additional term in eq (4) is included that  
 138 accounts for feedstock emissions. Emissions are then used to simulate atmospheric mole  
 139 fractions,  $MF_t$ , along with an assumed atmospheric lifetime,  $\tau_t$ , taken as the SPARC (2013)  
 140 multi-model time-varying mean;

$$141 \quad MF_{t+1} = \exp\left(\frac{-1}{\tau_t}\right) \times MF_t + A \times E_{\text{Total},t} \quad (5)$$

142 where A is a constant that converts units of emissions by mass to units of mole fractions, and  
 143 also takes into account a factor of 1.07 that accounts for the discrepancy between surface mole  
 144 fraction concentrations to global mean values.

## 145 2.2 Prior Distributions

146 The input parameters in the simulation model described above require initial values to be  
 147 assigned, along with their probability distributions. These prior distributions ('priors') are  
 148 developed to estimate mole fractions, emissions, and banks for CFC-11, 12, 113, 114, and 115,  
 149 HCFC-22, 141b, and 142b, and halon-1201, and 1311. Categories of bank equipment are  
 150 defined by the categorization provided by AFEAS (2001), which varies by compound (shown in  
 151 Table 1). For halons, there is a single category of bank (fire extinguishers).

152 AFEAS data reports global annual production up to 2001 categorized by equipment type,  
 153 which is generally categorized into short, medium and long-term banks. We use AFEAS data  
 154 and categorization to develop our production priors and adopt the WMO (2003) correction where  
 155 AFEAS production values are used up until 1989 and then scaled to match UNEP global  
 156 production values for all years following 1989. After AFEAS data ends, we assume the relative  
 157 production in each category remains constant for all years following 2001. Uncertainty in  
 158 production priors is assumed to follow a multivariate log-normal distribution, where temporal  
 159 correlation in production reporting bias is estimated in the BPE. Prior distributions differ by  
 160 chemical and are developed to be wide enough for atmospheric mole fraction priors to contain  
 161 observations. See the Supplement for details on production priors for each chemical.

162 The emissions function by bank equipment type can be characterized by the fraction of  
 163 production that is directly emitted during the year of production (DE) and the fraction of the  
 164 bank that is emitted in each subsequent year. Prior estimates for emissions functions come from  
 165 previously reported data and differ by chemical and equipment type (see the Supplement).  
 166 Broadly speaking, it has been estimated that chemicals contained in short-term banks are fully  
 167 emitted within the first two years after production, medium-term banks lose about 10 – 20% of  
 168 their material each year, and long-term banks can lose as little as 2% of their material each year  
 169 (Ashford et al., 2004). We use previously published estimates to develop emissions function  
 170 priors specific to each chemical and bank type along with wide uncertainties, as specified in the  
 171 Supplement.

172 Amounts of halocarbons used for feedstock production are available annually  
 173 (UNEP/TEAP, 2021). A prior mean leakage rate of 2% was assumed during production, which  
 174 reflects a medium value between different facilities (MCTOC, 2019).

175 **Table 1:** Application type of halocarbon banks by chemical

176 Chemical	177 Short Bank	178 Medium Bank	179 Long Bank
180 CFC-11	Aerosols	Non-hermetic refrigeration	Closed-cell foam

	Open-cell foam		
<b>CFC-12</b>	Aerosols Open-cell foam	Non-hermetic refrigeration	Refrigeration
<b>CFC-113</b>	solvents		Heat pump
<b>CFC-114</b>			Heat pump
<b>CFC-115</b>	Propellant		Air conditioning
<b>HCFC-22</b>	Open-cell foam	Non-hermetic refrigeration	Foam
<b>HCFC-141b</b>	Open-cell foam	Non-hermetic refrigeration	Foam
<b>HCFC-142b</b>		Non-hermetic refrigeration	Foam
<b>Halon-1211</b>		Fire extinguishers	
<b>Halon-1301</b>		Fire extinguishers	

181  
182  
183  
184  
185  
186

### 2.3 Likelihood function

For each chemical, the likelihood function is a multivariate normal likelihood function of the difference between modeled and observed mole fractions;

$$187 \quad P(D_{t1}, \dots, D_{tN} | \boldsymbol{\theta}) = \frac{1}{(2\pi)^{\frac{N}{2}} \sqrt{|S|}} \exp \left\{ -\frac{1}{2} \Delta^T S^{-1} \Delta \right\} \quad (6)$$

188  
189  
190  
191  
192  
193  
194  
195  
196  
197  
198  
199  
200  
201

Where  $D_{t1}, \dots, D_{tN}$  is yearly globally-averaged observed mole fractions for all years where observations are available and  $\boldsymbol{\theta}$  represents that vector of input and output parameters from the simulation model.  $\Delta$  is an  $N \times 1$  vector of the difference between yearly observed and modeled mole fractions and is assumed to have a mean zero, and covariance function  $S$ .  $S$  therefore represents the sum of uncertainties between observed and modeled mole fractions. While there are published estimates of uncertainties in observed mole fractions, we do not know the uncertainties in modeled mole fractions. Therefore, we estimate  $S$  separately for each chemical, as is done in (Lickley et al., 2020). The off-diagonals in the covariance function incorporate a correlation term,  $\rho_S$ , which accounts for our assumption that there is high autocorrelation in the bias between modeled and observed mole fractions. Correlation terms for each chemical are reported in the Supplement along with prior estimates of the uncertainty parameters used for diagonal elements in  $S$ . Each column and row in  $S$  is therefore populated as;

202  
203  
204  
205

$$S_{i,j} = \sigma_i \sigma_j \rho_S^{|i-j|}$$

where  $\sigma_i$  and  $\sigma_j$  represent the sum of the uncertainties in observed and modeled mole fractions at time  $i$  and  $j$ , respectively, and are inferred in the BPE, whereas  $\rho_S$  is prescribed.

206  
207  
208  
209  
210  
211  
212  
213

Observations come from the Advanced Global Atmospheric Gas Experiment (AGAGE; <https://agage.mit.edu>) data set (Prinn et al., 2000; Prinn et al., 2018), with the exception of CFC-11 and 12 which, following Lickley et al. (2021), come from the AGAGE and the National Oceanographic and Atmospheric Administration's (NOAA) merged data sets (Engel et al., 2019). Data are aggregated into annual global mean mole fractions. The time frame of availability of observations differs by chemical (see the Supplement).

### 2.4 Posterior Distributions

214 Following Bayes' Rule, we specify our posterior distribution as;

$$215 \quad 216 \quad P(\boldsymbol{\theta}|D_{t_1}, \dots, D_{t_N}) = \frac{P(\boldsymbol{\theta})P(D_{t_1}, \dots, D_{t_N}|\boldsymbol{\theta})}{P(D_{t_1}, \dots, D_{t_N})} \quad (7)$$

217  
218 Where  $P(\boldsymbol{\theta})$  represents the joint prior distribution of the input and output parameters described  
219 in the simulation model in Section 2.1.

220  
221 The analytical form of the posterior distribution is intractable. Thus, we estimate the posterior  
222 using a sampling procedure (the sampling importance resampling (SIR) method) to estimate the  
223 marginal posterior distributions (Bates et al., 2003; Hong et al., 2005; Rubin, 1988). To  
224 implement SIR we draw 1,000,000 samples from the priors, run the simulation model, and then  
225 resample from the priors 100,000 times using an importance ratio, which is proportional to the  
226 likelihood function. These sample sizes were chosen such that multiple iterations of the model  
227 produce consistent results.

228

### 229 3. Results

230 Figure 1 shows observed globally averaged mole fractions compared to BPE estimated mole  
231 fractions for each chemical. Figure 2 shows BPE estimated and observationally-derived  
232 emissions, assuming the SPARC time-varying multi-model mean lifetime for each species.  
233 Posterior estimates agree well with observations for the majority of time periods and chemicals.  
234 Note, however, that BPE estimates from Lickley et al. (2021) match observed and  
235 observationally-derived estimates more closely for CFC-11 than they do in the present analysis.  
236 We attribute this difference in consistency to atmospheric lifetimes being assumed in the present  
237 analysis, whereas they were inferred in Lickley et al. (2021), which found inferred lifetimes to be  
238 somewhat shorter than the SPARC multi-model mean values. Shorter lifetimes would allow  
239 modeled mole fractions to decline more quickly following 1990, better matching observations. A  
240 notable discrepancy occurs for CFC-115, where modeled mole fractions are increasing  
241 throughout the entire simulation period, whereas observed mole fractions from 2000 onwards are  
242 relatively constant. This discrepancy could be explained by the large uncertainties in  
243 atmospheric lifetimes of CFC-115 (Vollmer et al., 2018), if atmospheric lifetimes are in fact  
244 substantially shorter than the SPARC multi-model mean.

245

246 Figure 3 provides a comparison of BPE bank estimates alongside previously published bank  
247 estimates. BPE bank estimates are generally higher than other published values. This can be  
248 explained by production uncertainties that are accounted for in the present analysis. Our analysis  
249 suggests that production has very likely been underreported for nearly all chemicals. Table 2  
250 provides a summary of our estimated bias in cumulative reported production throughout the  
251 simulation period for each chemical type. With the exception of CFC-113 and CFC-115, we find  
252 our inferred cumulative production to be significantly higher than reported production (at the 1-  
253 sigma level), with our median estimate suggesting that production was as little as 9% higher than  
254 reported for CFC-12 and as high as 50% higher than reported for Halon-1211. We would expect  
255 any consistent bias in reported production to be a bias low, since consistent undercounting of  
256 production is more plausible than overcounting production. The exception for this would be the  
257 base year, which reduction targets are made with reference to. In this instance, we would expect  
258 overreporting for this year to be more likely. Another possible explanation for the discrepancy in  
259 production estimates is that total reported chemical production under the UNEP does not account

260 for leakage during chemical manufacturing, but rather only leakage that occurs during the  
 261 application of the chemical. To our knowledge, this potential leakage during chemical  
 262 manufacturing has not been well-documented or previously quantified.

263  
 264  
 265 **Table 2:** Estimated bias in cumulative reported production. Values indicate the percent  
 266 difference between inferred cumulative production from the onset of production to 2019 relative  
 267 to reported production, for all uses except for feedstock production. Positive values indicate the  
 268 percent by which inferred production is higher than reported.

Chemical Name	CFC-11	CFC-12	CFC-113	CFC-114	CFC-115
<b>Median inferred bias (16<sup>th</sup>, 84<sup>th</sup> percentile)</b>	12% (9%, 13%)	9% (7%, 11%)	-1% (-3%, 0%)	11% (9%, 13%)	-1% (-2%, 5%)
Chemical Name	HCFC-22	HCFC-141b	HCFC-142b	Halon-1211	Halon-1301
<b>Median inferred bias (16<sup>th</sup>, 84<sup>th</sup> percentile)</b>	10% (6%, 13%)	12% (6%, 19%)	22% (17%, 28%)	50% (41%, 59%)	24% (18%, 32%)

269  
 270  
 271 Figure 4 shows the breakdown of emissions by equipment type over time. For CFCs, emissions  
 272 from short-term banks tend to peak around 1990, as spray applications were banned earlier than  
 273 other applications, after which emissions from medium and long-term banks become more  
 274 dominant emission sources. This is to be expected as the phase-out of production after 1990  
 275 would lead to more CFC emissions from existing banks rather than new, short-lived equipment.  
 276 For HCFC-22, most of the emission throughout the entire time period is from medium banks,  
 277 which is largely non-hermetic refrigeration. Long banks (i.e. foams) dominate emissions for  
 278 HCFC-141b, and for HCFC-142b, where both foams and non-hermetic refrigeration are  
 279 prominent emission sources throughout the simulation period. Estimated feedstock emissions  
 280 averaged over 2010 – 2019 are shown in Table 3. HCFC-22 is the largest source of feedstock  
 281 emissions by mass, but CFC-113 feedstock emissions are estimated to be larger when weighted  
 282 by GWP100 and ODP.

283  
 284 **Table 3:** Estimated feedstock emissions averaged from 2010 – 2019 from the Bayesian analysis.  
 285 Emissions are weighted by mass, global warming potential (GWP100) relative to CO<sub>2</sub> over a  
 286 100-year time horizon for a CO<sub>2</sub> concentration of 391ppm, and by ozone depletion potential  
 287 (ODP) relative to CFC-11 (WMO, 2018).

Feedstock Emissions	CFC-113	HCFC-22	HCFC-142b
<b>By mass</b>	3.4 Gg/yr	9.3 Gg/yr	2.1 Gg/yr
<b>By GWP100</b>	20, 838 Gg/yr	16,591 Gg/yr	4,302Gg/yr
<b>By ODP</b>	2.8 Gg/yr	0.3 Gg/yr	0.1 Gg/yr

288  
 289 Figure 5 shows the relative quantity of banked materials by chemical type. Banks are weighted  
 290 by mass (Figure 5a), by global warming potential (GWP100; Figure 5b), and by ozone depleting  
 291 potential (ODP; Figure 5c). Our best estimate is that the sum of the HCFCs currently comprise  
 292 about 77% of banks by mass. However, in terms of climate impacts, CFC-11, 12 and HCFC-22  
 293 are the largest banked materials weighted by GWP100, accounting for 36%, 14%, and 36% of  
 294 current banks, respectively. When banks are weighted by ODP, CFC-11 and 12 represent 46%  
 295 and halons also represent 46% of current banked chemicals.

296

297 Figure 6 shows the composition of banks by chemical type. This, together with Figure 5,  
298 provides insight into the most prominent banked sources of halocarbons with regards to  
299 GWP100 and ODP. In terms of GWP100, CFC-11 banks largely reside in foams, whereas CFC-  
300 12 and HCFC-22 are largely in non-hermetic refrigeration; the latter may be more readily  
301 recoverable. In terms of ODP, CFC-11 foams and CFC-12 non-hermetic refrigeration remain  
302 important, along with halons which are all contained in fire extinguishers, a recoverable  
303 reservoir.

304  
305

#### 306 **4. Discussion and Conclusions**

307 This analysis suggests that if lifetime assumptions are correct, published bank estimates using  
308 either the top-down or bottom-up methods were likely underestimating bank sizes for all banked  
309 chemicals due to underreporting of production (see Table 2). The Bayesian approach used in this  
310 analysis does not assume production is known, but rather jointly infers production along with the  
311 other parameters in the simulation model, providing probabilistic estimates of historical  
312 production values. Previously published bank estimates (Ashford et al., 2004; TEAP, 2009;  
313 WMO, 2003) do not infer production, but rather assume it is known, or consider different  
314 scenarios. We argue that production assumptions have been biased low due to underreporting of  
315 total production and potentially unaccounted for leakage during chemical manufacturing and  
316 thus have led to published bank estimates that were also biased low.

317

318 Discrepancies between observed mole fractions and BPE-derived mole fractions are notable for  
319 the suite of chemicals considered here. While the majority fall within the 90% confidence  
320 interval throughout most of the time periods, the trends in concentrations between observations  
321 and inferred mole fractions do not always agree. This discrepancy could be related to our  
322 partitioning of production type following 2003 (i.e. after AFEAS data ends). Another important  
323 limitation in this analysis is in the treatment of atmospheric lifetimes, which could also explain  
324 some of these discrepancies. The present analysis assumes atmospheric lifetimes are known and  
325 equal to the SPARC (2013) time varying multi-model mean lifetimes. However, previous work  
326 has indicated potential biases in SPARC lifetimes, for example for CFCs (Lickley et al., 2021).  
327 The potential bias in atmospheric lifetimes would result in biased bank estimates in the present  
328 manuscript and requires further analysis.

329

330 This modeling approach makes no assumptions about end-of-life emissions. Certain bank  
331 estimates assume that applications are dismantled at the end of their lifetime, which would both  
332 contribute to decreased banks and increased emissions at fixed years after production (e.g. TEAP  
333 progress report, 2021). We do not make this assumption as we believe it would be more realistic  
334 for dismantling of equipment to occur over a range of years after production, which would  
335 effectively be captured by our bank release fraction estimate. We do, however, test the  
336 sensitivity of our bank estimate to end-of-life (EOL) emissions occurring in a single year after  
337 production. This we term the EOL scenario and test the sensitivity of banks for CFC-11, CFC-  
338 12 and HCFC-22, the three largest banks by global warming potential. The modeling approach  
339 is described in the SM and results are shown in Figure SM1. Perhaps unexpectedly, CFC-11  
340 posterior bank estimates are ~25% higher in 2020 in the EOL scenario relative to the scenario  
341 described in the main text. However, banks in the EOL scenario are decreasing faster than those  
342 described in the main text. The larger bank size is due to posterior bank release fractions being ~



343 2% for the EOL scenario relative to 3% for the scenario described in the main text. The faster  
344 depletion of the banks in 2020 can be explained by the addition of the EOL decommissioning  
345 parameter. These larger bank estimates reflect the consistency of the Bayesian modeling  
346 approach where all parameters are jointly inferred. Including an additional process in the model  
347 requires that multiple parameters be updated to be consistent with observations. For CFC-12, the  
348 EOL scenario produces significantly smaller banks from about 1990 onwards, however, the  
349 emissions profile has an artificial dip in emissions relative to observationally-derived emissions,  
350 suggesting a set year for decommissioning is not a realistic modeling assumption. For HCFC-22  
351 banks are not substantially different between the two scenarios.

352  
353 There are important discrepancies between CFC-113 feedstock emissions inferred here and those  
354 estimated in the previous analysis (Lickley et al., 2020). In Lickley et al. (2020), feedstock  
355 emissions were assumed to be the difference between observationally-derived emissions and  
356 inferred bank emissions. In the present analysis, prior distributions of feedstock production and  
357 leakage rates are developed and feedstock emissions are then inferred. In the present analysis,  
358 observationally-derived CFC-113 emissions are higher than total BPE inferred emissions at the  
359 1-sigma level from 2010 onwards. This suggests that either observationally-derived emissions  
360 are too high, or our BPE estimates are too low. In Lickley et al. (2021), we find that atmospheric  
361 lifetimes of CFC-113 are very likely lower than the SPARC multi-model time varying mean,  
362 used in the present analysis. This would imply that the observationally-derived emissions shown  
363 in Figure 2 are biased low, suggesting an even larger discrepancy between BPE inferred total  
364 emissions and observationally derived emissions. Therefore, it seems plausible that the  
365 discrepancy is due to prior feedstock emissions estimates being biased low due to larger leakage,  
366 or CFC-113 is being produced for a use that is not allowed under the Montreal Protocol.

367  
368 Finally, some important details about production and destruction were not fully accounted for in  
369 this analysis. For one, feedstock priors were only included for CFC-113, HCFC-22, and HCFC-  
370 142b, which could be limiting our assessment of the sources of emissions for other chemicals.  
371 However, published feedstock values for other chemicals are not available and leakage rates in  
372 feedstock applications may be uncertain. In addition, we do not account for non-dispersive  
373 production in our analysis, namely the production of chemicals as by-products. It is possible, for  
374 example, that some of the discrepancies in CFC-115 emissions could be explained by non-  
375 dispersive emissions as identified by (Vollmer et al., 2018). Further, we do not consider end-of-  
376 life destruction of equipment as there are no published records, to our knowledge, of these  
377 processes. Finally, we were not able to account for a more detailed breakdown in production by  
378 equipment type than what has been published by AFEAS, which discretizes production into, at  
379 most, four categories of equipment, and does not provide data beyond 2003. Without publicly  
380 available details of these processes, modeling of banks and emissions will continue to be limited.

381  
382 **Code Availability:** All analyses were done in MATLAB. All code used in this work is available  
383 at <https://github.com/meglickley/HalocarbonBanks>

384  
385 **Data Availability:** The datasets generated and/or analyzed during the current study are available  
386 at <https://github.com/meglickley/HalocarbonBanks>

387

388 **Author Contributions.** All authors contributed to the conceptualization of the manuscript.  
389 M.L. conducted the analysis. M.L. prepared the manuscript with contributions from all authors.

390  
391 **Competing Interests.** The authors declare that they have no conflict of interest.

392  
393 **Acknowledgements.** M.L. and S.S. gratefully acknowledge the support of VoLo foundation  
394 and grant 2128617 from the atmospheric chemistry division of NSF. AGAGE is supported  
395 principally by NASA (USA) grants to MIT and SIO, and also by: BEIS (UK) and NOAA (USA)  
396 grants to Bristol University; CSIRO and BoM (Australia); FOEN grants to Empa (Switzerland);  
397 NILU (Norway); SNU (Korea); CMA (China); NIES (Japan); and Urbino University (Italy). E.F.  
398 acknowledges support of the NASA Headquarters Atmospheric Composition Modeling and  
399 Analysis Program.

400  
401

## 402 **References**

- 403 AFEAS. (2001). AFEAS 2001 database. Retrieved from  
404 [https://unfccc.int/files/methods/other\\_methodological\\_issues/interactions\\_with\\_ozone\\_layer](https://unfccc.int/files/methods/other_methodological_issues/interactions_with_ozone_layer/application/pdf/cfc1100.pdf)  
405 [/application/pdf/cfc1100.pdf](https://unfccc.int/files/methods/other_methodological_issues/interactions_with_ozone_layer/application/pdf/cfc1100.pdf)
- 406 Andersen, S. O., Metz, B., Kuijpers, L., & Solomon, S. (Eds.). (2005). *Safeguarding the Ozone*  
407 *Layer and the Global Climate System: Special Report of the Intergovernmental Panel on*  
408 *Climate Change*. Cambridge University Press.
- 409 Ashford, P., Clodic, D., McCulloch, A., & Kuijpers, L. (2004). Emission profiles from the foam  
410 and refrigeration sectors comparison with atmospheric concentrations. Part 1: Methodology  
411 and data. *International Journal of Refrigeration*, 27(7), 687–700.
- 412 Bates, S. C., Cullen, A., & Raftery, A. E. (2003). Bayesian uncertainty assessment in  
413 multicompartment deterministic simulation models for environmental risk assessment.  
414 *Environmetrics: The Official Journal of the International Environmetrics Society*, 14(4),  
415 355–371.
- 416 Engel, A., Rigby, M., Burkholder, J. B., Fernandez, R. P., Froidevaux, L., Hall, B. D., et al.  
417 (2019). *Update on Ozone-Depleting Substances (ODSs) and other gases of interest to the*  
418 *Montreal Protocol, Chapter 1 in Scientific Assessment of Ozone Depletion: 2018, Global*  
419 *Ozone Research and Monitoring Project - Report No. 58*. Geneva, Switzerland: World  
420 Meteorological Organization.
- 421 Gamlen, P. H., Lane, B. C., Midgley, P. M., & Steed, J. M. (1986). The production and release to  
422 the atmosphere of CCl<sub>3</sub>F and CCl<sub>2</sub>F<sub>2</sub> (chlorofluorocarbons CFC11 and CFC 12).  
423 *Atmospheric Environment*, 20(6), 1077–1085.
- 424 Hong, B., Strawderman, R. L., Swaney, D. P., & Weinstein, D. A. (2005). Bayesian estimation  
425 of input parameters of a nitrogen cycle model applied to a forested reference watershed,  
426 Hubbard Brook Watershed Six. *Water Resources Research*, 41(3).
- 427 IPCC/TEAP. (2006). *Task Force on Emissions Discrepancies Report, Technical Report*. Nairobi,  
428 Kenya.
- 429 Lickley, M., Solomon, S., Fletcher, S., Rigby, M., Velders, G. J. M., Daniel, J., et al. (2020).  
430 Quantifying contributions of chlorofluorocarbon banks to emissions and impacts on the  
431 ozone layer and climate. *Nature Communications*, 11(1380).  
432 <https://doi.org/10.1038/s41467-020-15162-7>
- 433 Lickley, M., Fletcher, S., Rigby, M., & Solomon, S. (2021). Joint Inference of CFC lifetimes and

434 banks suggests previously unidentified emissions. *Nature Communications*, 12(2920), 1–10.  
435 <https://doi.org/https://doi.org/10.1038/s41467-021-23229-2> |

436 MCTOC. (2019). *Medical and Chemical Technical Options Committee, 2018 assessment*.  
437 Retrieved from [https://ozone.unep.org/sites/default/files/2019-04/MCTOC-Assessment-](https://ozone.unep.org/sites/default/files/2019-04/MCTOC-Assessment-Report-2018.pdf)  
438 [Report-2018.pdf](https://ozone.unep.org/sites/default/files/2019-04/MCTOC-Assessment-Report-2018.pdf)

439 Montzka, S. A., Dutton, G. S., Yu, P., Ray, E., Portmann, R. W., Daniel, J. S., et al. (2018). An  
440 unexpected and persistent increase in global emissions of ozone-depleting CFC-11. *Nature*,  
441 557(7705), 413.

442 Newman, P. A., Oman, L. D., Douglass, A. R., Fleming, E. L., Frith, S. M., Hurwitz, M. M., &  
443 Kawa, S. R. (2009). What would have happened to the ozone layer if chlorofluorocarbons  
444 (CFCs) had not been regulated? *Atmospheric Chemistry and Physics*, 9(6), 2113–2128.

445 Poole, D., & Raftery, A. E. (2000). Inference for deterministic simulation models: the Bayesian  
446 melding approach. *Journal of the American Statistical Association*, 95(452), 1244–1255.

447 Prinn, R. G., Weiss, R. F., Fraser, P. J., Simmonds, P. G., Cunnold, D. M., Alyea, F. N., et al.  
448 (2000). A history of chemically and radiatively important gases in air deduced from  
449 ALE/GAGE/AGAGE. *Journal of Geophysical Research Atmospheres*, 105(D14), 17751–  
450 17792. <https://doi.org/10.1029/2000JD900141>

451 Prinn, Ronald G., Weiss, R. F., Arduini, J., Arnold, T., Langley Dewitt, H., Fraser, P. J., et al.  
452 (2018). History of chemically and radiatively important atmospheric gases from the  
453 Advanced Global Atmospheric Gases Experiment (AGAGE). *Earth System Science Data*,  
454 10(2), 985–1018. <https://doi.org/10.5194/essd-10-985-2018>

455 Rubin, D. B. (1988). Using the SIR algorithm to simulate posterior distributions (with  
456 discussion). *Bayesian Statistics*, 3, 395–402.

457 SPARC. (2013). SPARC Report on the Lifetimes of Stratospheric Ozone-Depleting Substances,  
458 Their Replacements, and Related Specied. (M. Ko, P. Newman, S. Reimann, & Strahan S.,  
459 Eds.). SPARC Report N. 6, WCRP-15/2013.

460 TEAP. (2009). *TEAP (Technology and Economic Assessment Panel), Task Force Decision XX/8*  
461 *Report, Assessment of Alternatives to HCFCs and HFCs and Update of the TEAP 2005*  
462 *Supplement Report Data*. Nairobi, Kenya. Retrieved from  
463 [http://ozone.unep.org/teap/Reports/TEAP\\_%0AReports/teap-may-2009-decisionXX-8-task-](http://ozone.unep.org/teap/Reports/TEAP_%0AReports/teap-may-2009-decisionXX-8-task-forcereport.%0Apdf)  
464 [forcereport.%0Apdf](http://ozone.unep.org/teap/Reports/TEAP_%0AReports/teap-may-2009-decisionXX-8-task-forcereport.%0Apdf)

465 UNEP/TEAP. (2021). *TEAP Progress Report Volume I*. Nairobi, Kenya. Retrieved from  
466 <https://ozone.unep.org/system/files/documents/TEAP-2021-Progress-report.pdf>

467 Velders, G. J. M., & Daniel, J. S. (2014). Uncertainty analysis of projections of ozone depleting  
468 substances: mixing ratios, EESC, ODPs, and GWPs. *Atmospheric Chemistry and Physics*,  
469 14(6), 2757–2776.

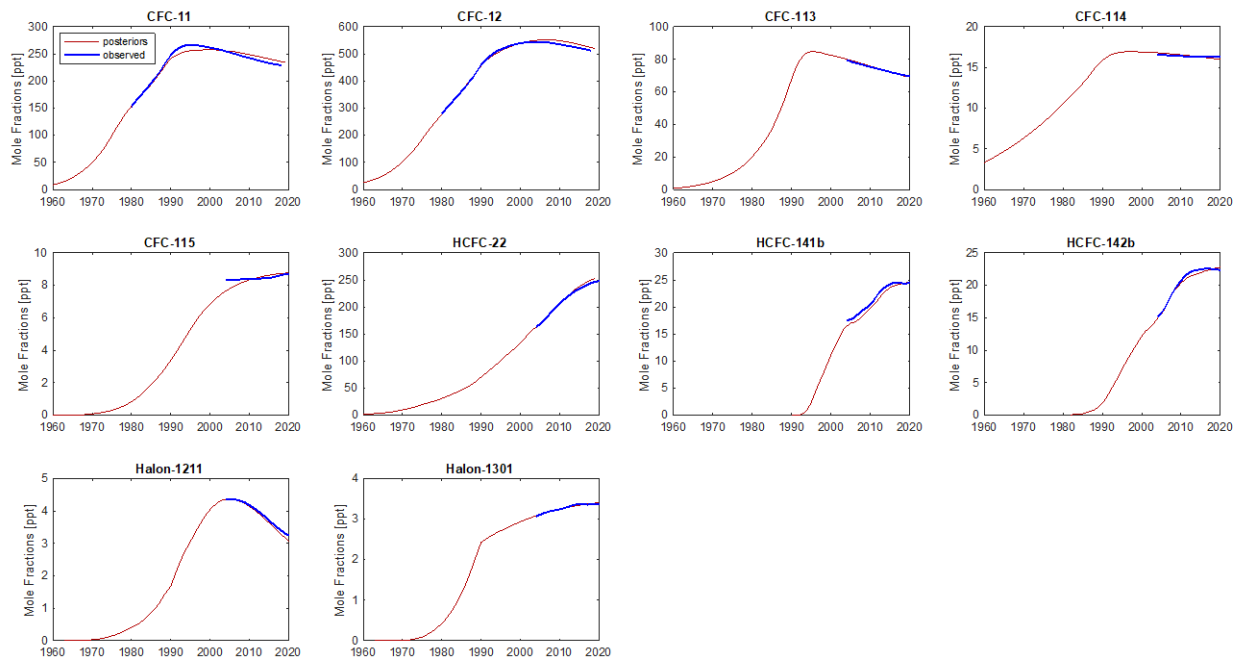
470 Vollmer, M. K., Young, D., Trudinger, C. M., Mühle, J., Henne, S., Rigby, M., et al. (2018).  
471 Atmospheric histories and emissions of chlorofluorocarbons CFC-13 (CClF3),  $\Sigma$ CFC-114  
472 (C2Cl2F4), and CFC-115 (C2ClF5). *Atmospheric Chemistry and Physics*, 18(2), 979–1002.  
473 <https://doi.org/10.5194/acp-18-979-2018>

474 WMO. (2003). WMO: Scientific Assessment of Ozone Depletion: 2002, Global Ozone Research  
475 and Monitoring Project – Report No. 47. Geneva, Switzerland: World Meteorological  
476 Organization (WMO),.

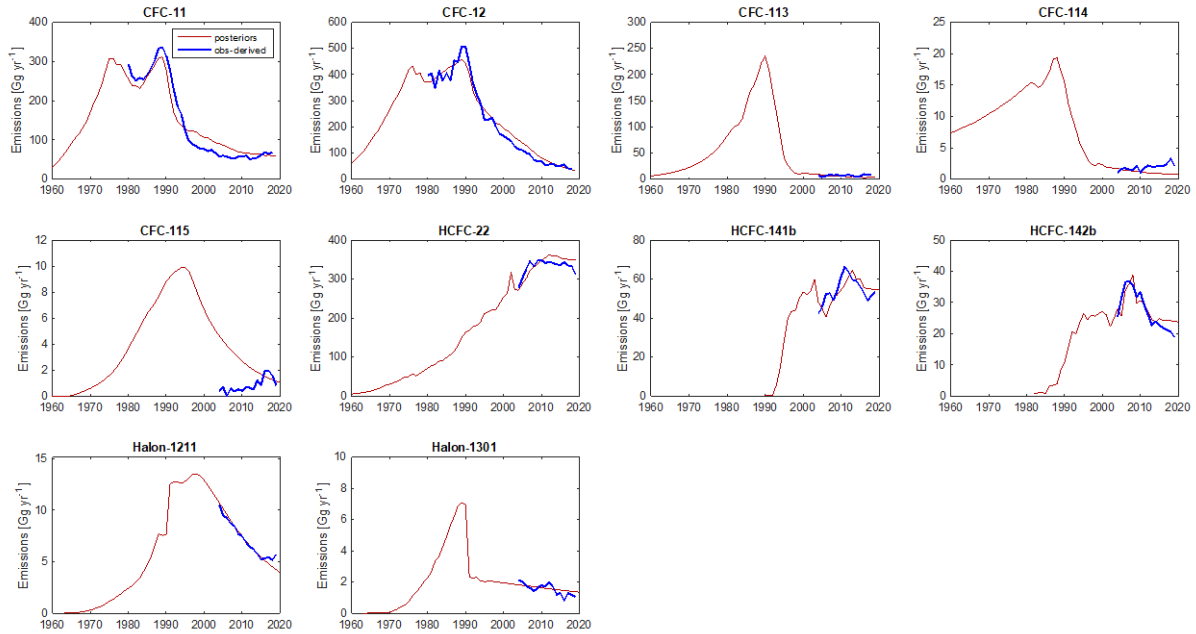
477 WMO. (2011). *Scientific Assessment of Ozone Depletion: 2010, Global Ozone Research and*  
478 *Monitoring Project-Report No. 52*. Geneva, Switzerland.

479 WMO. (2014). *Scientific Assessment of Ozone Depletion: 2014, World Meteorological*

480 *Organization, Global Ozone Research and Monitoring Project-Report No. 55. Geneva,*  
481 *Switzerland.*  
482 WMO. (2018). WMO: Scientific Assessment of Ozone Depletion: 2018, Global Ozone Research  
483 and Monitoring Project – Report No. 58. Geneva, Switzerland: World Meteorological  
484 Organization (WMO),.  
485  
486  
487

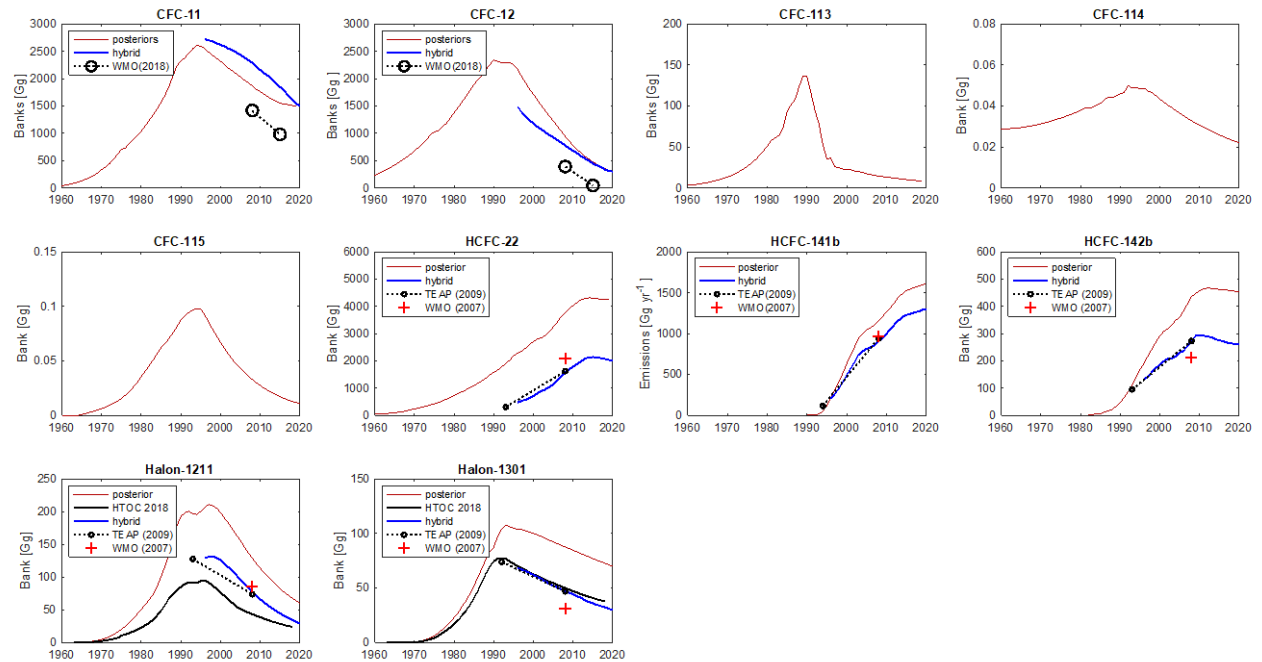


488 **Figure 1:** Modeled mole fractions versus observed mole fractions. Red lines indicate the  
489 posterior median mole fraction estimate from the Bayesian analysis (BPE), with shaded regions  
490 indicating the 90% confidence interval. Blue line indicates globally-averaged observed mole  
491 fractions.  
492  
493



494  
495  
496  
497  
498  
499  
500

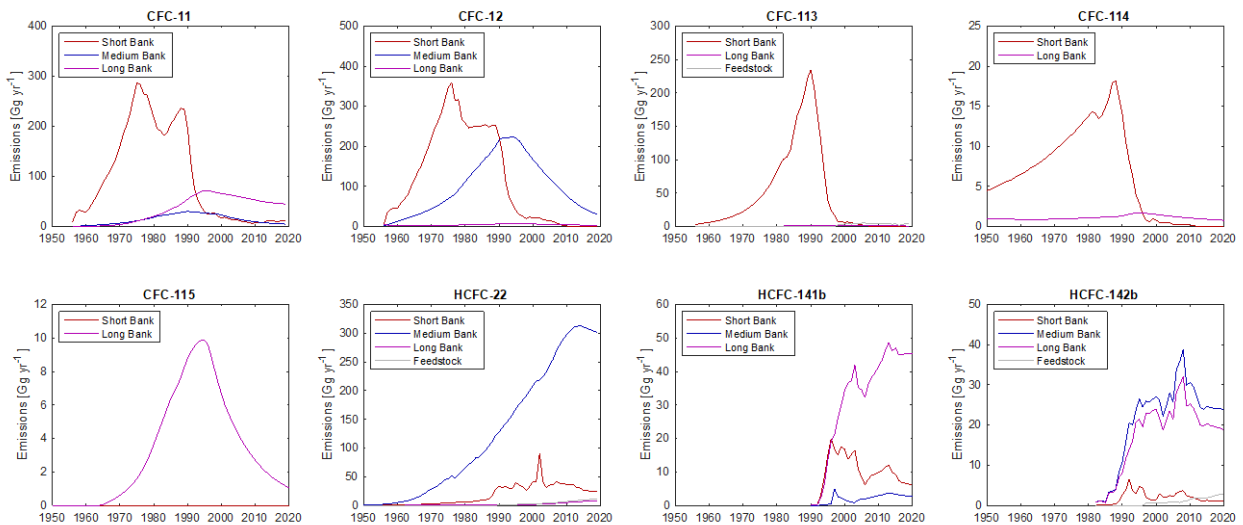
**Figure 2:** Modeled emissions versus observationally-derived emissions. Red lines indicate the posterior median emissions estimate from the Bayesian analysis (BPE), with shaded regions indicating the 90% confidence interval. Blue line indicates observationally-derived emissions assuming the SPARC multi-model mean time-varying lifetimes.



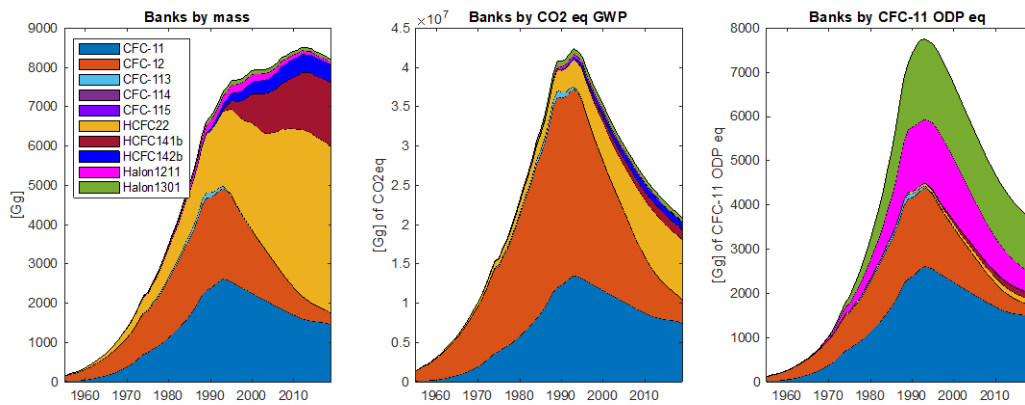
501  
502  
503  
504

**Figure 3:** Magnitudes of Bank estimates. The red line indicates the median posterior estimate of Banks from the Bayesian analysis, with shading indicating the 90% confidence interval. Previously published bank estimates are provided for comparison from TEAP (2009), WMO

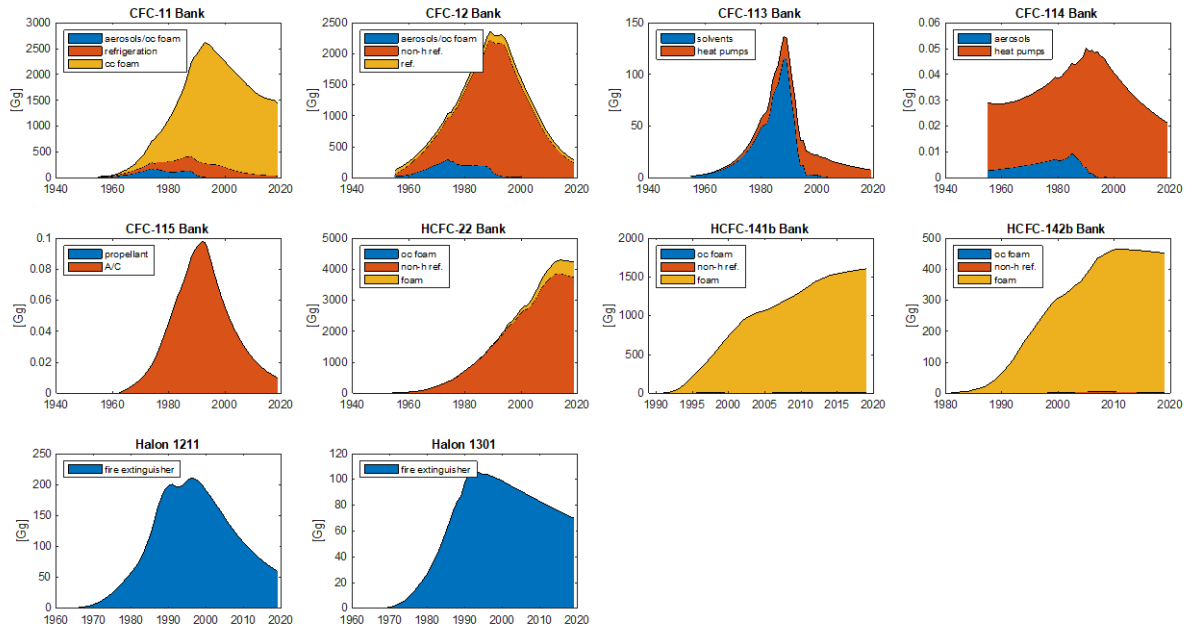
505 (2007), and WMO (2018), along with the hybrid approach updated to current estimated starting  
 506 values.  
 507



508  
 509 **Figure 4:** Emissions by Source. Emissions estimates by various equipment types, summarized  
 510 in Table 1, are shown here along with estimated emissions from feedstock usage. Lines indicate  
 511 the median estimate, with the shaded region indicating the 90% confidence interval. Halons are  
 512 not included in this figure as 100% of halon emissions come from the same application and are  
 513 thus identical to Figure 2 halon totals.



514  
 515 **Figure 5:** Total banks by mass, global warming potential (GWP100; WMO, 2018) and ozone  
 516 depleting potential (ODP; WMO, 2018). Bank estimates reported in the above figures are the  
 517 median estimates from the Bayesian analysis.  
 518



519  
 520  
 521  
 522  
 523  
 524

**Figure 6:** Bank size by equipment type. Bank estimates reported in the above figures are the median estimates from the Bayesian analysis. In the above legends, cc refers to closed-cell foams, non-h ref. refers to non-hermetic refrigeration, ref. refers to refrigeration, and A/C refers to air conditioning.